J Sol-Gel Sci Technol (2013) 68:67–74
DOI 10.1007/s10971-013-3135-1

ORIGINAL PAPER

Low-temperature versus oxygen plasma treatment of water-based TiO_2 paste for dye-sensitized solar cells

Mateja Hočevar · Urša Opara Krašovec · Marko Topič

Received: 11 June 2013 / Accepted: 30 July 2013 / Published online: 7 August 2013

Abstract High-temperature treatment steps in fabrication process of dye sensitized solar cell (DSSC) significantly contribute to the manufacturing costs and limit the use of temperature sensitive substrates. Therefore our aim was to develop a simple method for the preparation of water-based TiO_2 paste. The paste is based on peroxotitanic acid (PTA) sol–gel matrix and commercial TiO_2 nanoparticles (P25). Two fabrication processes to decompose/transform the PTA matrix in the printed TiO_2 layer are explored and combined: annealing at temperatures up to 250 °C and/or oxygen plasma treatment. The results show that the PTA matrix in the paste converts to anatase phase and to some extent also attaches to the TiO_2 nanoparticles P25 acting as an interconnecting network within TiO_2 layer. The transformation of the PTA matrix occurs around 250 °C, but in the presence of TiO_2 nanoparticles P25 it starts already at 120 °C. In addition the results reveal that the crystallization is achievable also solely with the oxygen plasma treatment. The efficiency of the TiO_2 layers, exposed to different post-deposition treatments, is evaluated in DSSCs. The results show that oxygen plasma treatment of the TiO_2 layers could efficiently replace temperature curing at 250 °C. Within this study the DSSCs with the efficiency up to 4.2 % measured under standard test conditions (1,000 W/m^2, AM1.5, 25 °C) were realized.

Keywords Peroxotitanic acid · Sol–gel · TiO_2 paste · Low-temperature treatment · Oxygen plasma treatment · Dye-sensitized solar cell

M. Hočevar (✉) · U. Opara Krašovec · M. Topič
Faculty of Electrical Engineering, University of Ljubljana, Tržaška cesta 25, 1000 Ljubljana, Slovenia
e-mail: mateja.hocevar@fe.uni-lj.si

1 Introduction

Dye-sensitized solar cells (DSSCs) [1], due to their potential low-cost manufacturing process based on screen printing technology and optical semi-transparency along with decorative options, offer multiple opportunities for the architectural solutions for envelope of modern buildings [2, 3]. In the last decade the research in the field of DSSCs has been focusing on glass-substrate solar cells, although flexible substrates (polymer foils) enable a wider range of applications which could foster this technology towards its industrialization [4, 5]. Recently a strong emphasis has been given to the development of low-temperature pastes for DSSCs fabrication in order to avoid conventional high-temperature curing (above 400 °C). The main advantages are low-cost, light-weight, flexible devices and roll-to-roll manufacturing [6–9]. However, one of the problems of using a polymer substrate in DSSCs is that the solar cells exhibit a lower conversion efficiency up to 7.6 % [10], while the record efficiency of the glass-based DSSC exceeds 12.3 % [11]. One of the main reasons for this is the limitation of the annealing temperature of the TiO_2 layer up to 250 °C which does not enable optimal interconnection of the TiO_2 nanoparticles within the layer necessary for good electron transport within photoactive layer [12].

Several efforts have been made towards low-temperature preparation of the active layer focusing on the preparation of the binder-free TiO_2 pastes [13, 14], using a mixture of nanocrystalline TiO_2 powder and titania precursor with the UV irradiation treatment [15] or hydrothermal crystallization at low temperature in the solid/gas interface [16]. Li et al. [17] developed low temperature fabrication method for the preparation of active layer by blending of poly(methyl methacrylate) with TiO_2 nanoparticles. The flexibility of

photoelectrode has been improved, although the efficiency of DSSC was decreased by the presence of polymer in TiO_2 layer. Lindström et al. [18, 19] introduced the press method for low-temperature preparation of the TiO_2 electrodes. Using electrodes prepared by this method, they achieved the efficiency up to 3 % [19]. Dürr et al. [20] developed a lift-off process. The TiO_2 layer was deposited on gold-layered glass substrate and sintered at high temperatures. Afterwards, the TiO_2 layer was removed from the glass by dissolving the gold layer. The TiO_2 layer was transferred onto a conductive plastic substrate by pressing. By this process an efficiency of 5.8 % has been achieved. The most promising research results were published by Yamaguchi et al. [10]; they reported highly efficient (7.6 %) DSSC based on plastic substrate using a press method. The high conversion efficiency was achieved by optimization of the press conditions, improving of the low-temperature TiO_2 paste and an additional UV–O_3 treatment of the TiO_2 layer and the plastic substrate [10].

The procedures for the fabrication of TiO_2 layer for the plastic DSSCs are rather complex. Therefore, our aim was to simplify the preparation of the TiO_2 paste which allows the formation of TiO_2 layers at low temperatures ($\leq$250 °C). To accomplish this goal, a TiO_2 paste based on the water-based sol–gel matrix and commercial TiO_2 nanopowder has been successfully developed. The matrix was synthesized by mixing Ti-isopropoxide (Ti(O*i*Pr)$_4$) and hydrogen peroxide (H_2O_2) forming complexing gel called peroxotitanic acid (PTA) [21]. The TiO_2 paste was achieved by mixing the sol–gel matrix and commercial TiO_2 nanopowder. The PTA crystallizes at rather low temperature, therefore we assume that the PTA present in the paste at low temperature converts to small TiO_2 crystals and to some extent also attaches to the basic TiO_2 nanopowder and acts as an interconnecting network within TiO_2 layer. A similar approach has been reported by Yen et al. [13], who introduced PTA and tert-butyl alcohol into the paste based on a mixture of nanocrystalline powder P25, P90 and PT501A. They prepared the TiO_2 layers by temperature curing at 120 °C for 4 h. Our aim was to simplify the synthesis of TiO_2 paste and at the same time efficiently replace temperature curing with plasma treatment and significantly shorten the processing time of TiO_2 layer preparation. Two routes have been explored and also combined: annealing at low temperature ($\leq$250 °C) and/or treating with the oxygen plasma to study the transformation of the PTA in the printed TiO_2 layer. Plasma treatment is commonly used for cleaning, etching, activating and functionalizing a variety of surfaces (polymeric materials, metal, plastic, etc.) [22–26]. Plasma treatment has already been used for the preparation of DSSC, mostly for the cleaning and activating of the substrate before depositing of TiO_2 layer to improve adhesion. Recently some efforts have been already made towards a surface-treatment of photoactive electrodes (TiO_2 layers) to increase the dye absorption and improve the performance of DSSCs [27–30]. Our aim was to replace or combine temperature curing with oxygen plasma treatment.

Newly developed water-based TiO_2 matrix/paste/layers have been thoroughly studied. Ten different combinations of post-deposition treatments of the TiO_2 layers composed of the water-based sol–gel matrix and TiO_2 nanopowder have been explored. The sol–gel matrix and the TiO_2 paste have been examined with the infrared spectroscopy (IR). The differences in TiO_2 layer structure and morphology upon the different treatments of the as-deposited layers have been described by the X-ray diffraction (XRD) and scanning electron microscopy (SEM). The amount of the dye molecules attached to the TiO_2 layer has been determined with the UV–Vis spectroscopy. Additionally, the TiO_2 layers have been used to assemble a series of DSSCs. The incident photon to current efficiency (IPCE) of DSSCs employing TiO_2 layers exposed to different treatments, as well as the cells performance under standard test conditions (STC; 1,000 W/m^2, AM1.5, 25 °C) have been evaluated. The efficiency of the ten different TiO_2 layers in DSSC has been compared using an ionic liquid based electrolyte. Nevertheless in general the DSSCs based on this type of electrolyte show diffusion limitation which is reflected in lower efficiency of the solar cell [31]. Therefore the most efficient TiO_2 layer has been tested also in the DSSC based on acetonitrile electrolyte.

2 Experimental

2.1 Preparation of the TiO_2 paste

The first step in the preparation of TiO_2 paste was the synthesis of peroxotitanic acid (PTA) sol–gel matrix. The matrix was achieved by mixing Ti(O*i*Pr)$_4$ (Fluka) and H_2O_2 (30 % aqueous solution, Belinka). The optimal molar ratio between Ti(O*i*Pr)$_4$ and H_2O_2 was found to be 1:30. The H_2O_2 was added drop-wise to Ti(O*i*Pr)$_4$, meanwhile the mixture generated heat, evolved oxygen bubbles and transformed into red–yellow complex. Afterwards, the remaining H_2O_2 was added to the mixture and a yellow gel called peroxotitanic acid (PTA), denoted as matrix, was formed.

The TiO_2 paste was prepared by mixing the TiO_2 nanopowder (P25, Degussa) and PTA gel in a mortar grinder (Retsch, RM200). The molar ratio between TiO_2 and Ti(O*i*Pr)$_4$ in the paste was 7:1, since our previous study has shown that this is the most suitable molar ratio in the paste concerning the optimal DSSC performance [32]. The mixture was stirred and the distilled H_2O was added slowly till a homogeneous paste was obtained.

2.2 Preparation of the TiO_2 layer

The TiO_2 paste was deposited on a transparent conductive electrode (TCO) i.e. fluorine-doped SnO_2 on glass substrate (TEC8, Solaronix, 8 Ohm/square), using the "doctor blade" technique. Afterwards, the printed TiO_2 layers were exposed to different conditions;

1. air drying at room temperature (marked as layer RT),
2. treating at different temperature–time combinations: 15 h at 120 °C (layer T120), 15 h at 180 °C (layer T180), 1 h at 250 °C (layer T250′), 15 h at 250 °C (layer T250) and 1 h at 450 °C (layer T450′),
3. treating with oxygen plasma (layer P-RT),
4. annealing followed by oxygen plasma treatment: 1 h at 120 °C (layer P120′), 1 h at 180 °C (layer P180′) and 1 h at 250 °C (layer P250′).

We used a cylindrical plasma reactor developed by and in-operation at the Jožef Stefan Institute [33]. The plasma process was carried out at a pressure of 30 Pa and power of 3.2 kW for 6 min in pure O_2. More details about the oxygen plasma treatment can be found in [33].

2.3 Fabrication of the DSSC

The cells were assembled in accordance with the standard procedure as reported previously [32, 34]. The TiO_2 layers were immersed in an ethanol solution of the ruthenium complex dye N719 (1×10^{-4} M, Ru (2,2′ bipyridy l4, 4′ dicarboxylate)$_2$ $(NCS)_2$, Solaronix). Two different electrolytes were used; electrolyte A was based on a binary ionic liquid mixture and electrolyte B was based on acetonitrile. Electrolyte A consisted of 1-propyl-3-methyl-imidazolium iodide (Merck) and 1-ethyl-3-methyl-imidazolium tetracyanoborate (Merck) mixed in volume ratio 13:7, 0.2 M iodine (Merck), 0.5 M 1-methylbenzimidazole (Aldrich) and 0.1 M guanidine thiocyanate (Fluka). Electrolyte B consisted of 0.6 M 1-propyl-3-methyl-imidazolium iodide, 0.03 M iodine, 0.1 M guanidine thiocyanate, 0.5 M 4-*tert*-butylpiridine (Aldrich) in acetonitrile (Riedel-de Haën). The active area of DSSCs was 0.3 cm^2.

2.4 Instrumental and measuring techniques

The layer thickness was determined with surface profilometer (Taylor-Hobson Ltd.).

The IR spectra of the PTA, TiO_2 paste and TiO_2 powder were recorded using a FT-IR spectrometer Spectrum GX, ATR technique.

The XRD measurements of dried PTA gel and TiO_2 layers were done using a Phillips PW1710 (automated) X-ray diffractometer. Before XRD characterisation the PTA gel were annealed at different temperatures: air drying at room temperature (G-RT), 15 h at 120 °C (G120), 15 h at 180 °C (G180), 1 h at 250 °C (G250′), 15 h at 250 °C, (G250) and 1 h at 450 °C (G450′). The XRD measurements were also done for the layers RT, P-RT and T250 deposited on TCO substrates.

The surface morphology of the layers was analysed with FEI Helios Nanolab 650 scanning electron microscope (SEM).

The amount of the dye molecules adsorbed on the TiO_2 layer, which correlates with the active surface area of the TiO_2 layer, was determined with UV–Vis spectroscopy. Detailed procedures for the determination of amount of the dye adsorbed on the TiO_2 layers have been described previously [35, 36].

Oriel Class ABA solar simulator (equipped with 1.5G air mass filter) was used as the light source. Although it's spectrum closely matches required AM1.5 spectrum according to the IEC 60904-3 standard, the spectral mismatch parameter was calculated and used in conjunction with a calibrated c-Si reference solar cell. To set the cell temperature to the standard test conditions (25 °C), the temperature was stabilized with a cooling/heating setup based on Peltier element designed for solar cell characterization. Current–voltage (*I/V*) characteristics were measured using a precise source meter by applying voltage and measuring current.

The IPCE of the assembled DSSCs was analysed with a Xenon lamp and a monochromator. The measurement were scanned in increments of 5 nm from 300 to 800 nm, while in order to obtain stable reading the 3 s delay was applied after setting wavelength and before measurement of the current.

3 Results and discussion

The layers are marked upon the different treatments of the as-deposited layers (see experimental), while the solar cells are marked as $DSSC_{layer}$ (e.g. $DSSC_{RT}$) according to the type of the TiO_2 layer used.

3.1 Structure and morphology of PTA, TiO_2 paste and TiO_2 layer

3.1.1 IR spectroscopy

Figure 1 shows the FT-IR spectra of the TiO_2 paste and its precursors; PTA gel (matrix) and TiO_2 nanopowder (P25). The spectrum of the PTA and TiO_2 paste are characterised with a wide absorption from 3,000 to 3,700 cm^{-1} related to the stretching vibration of the hydrogen-bonded OH groups of the adsorbed water. The absorption around 1,630 cm^{-1} can be assigned to the bending vibration of adsorbed H_2O

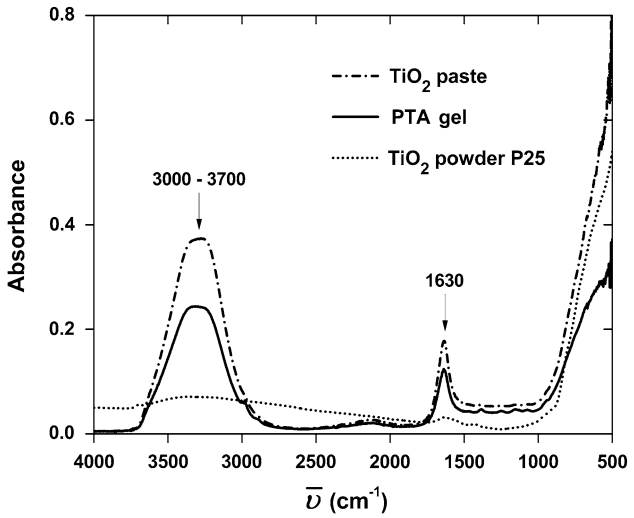

Fig. 1 The FT-IR spectra of TiO_2 paste, PTA gel and TiO_2 powder P25

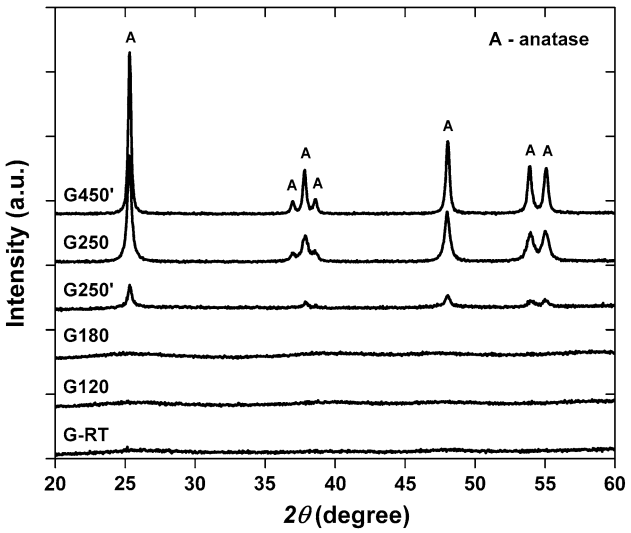

Fig. 2 XRD patterns of PTA gel annealed at different temperatures

molecules. The stretching vibrations assigned to the peroxo group (-Ti–O–O–H) bond of the peroxotitanic acid (PTA) are typically present at 900 cm^{-1} [37, 38], however this absorption peak is not present in the spectrum of the PTA gel (Fig. 1). The $Ti_4{}^+$ ions and H_2O_2 interaction leading to the formation of a Ti-peroxy compound is exothermic. We assume that in our case the peroxo groups were decomposed, either because the synthesis was not performed under ice-bath conditions and/or since the PTA gel was air-dried at room temperature for 2 days before the FT-IR measurements were taken. Nevertheless, Ge et al. also observed completely decomposition of peroxo group in PTA after treatment at 100 °C for 6 h [37]. It should be mentioned that in their case other precursors (titanyl sulfate, ammonia) and different synthesis routes have been used for the preparation of the PTA. For the TiO_2 powder (P25), the bands near 1,630 cm^{-1} and 3,000–3,700 cm^{-1} also show the presence of O–H bonds. This is probably due to the fact that the TiO_2 easily adsorbs water vapor from the air, leading to the formation of hydroxyl groups on the surface of the TiO_2 [38]. In general, FT-IR analysis (Fig. 1) revealed that there is no chemical interaction between PTA gel and TiO_2 powder P25, since the FT-IR spectrum of the TiO_2 paste is a sum of the IR spectrum of the PTA gel and TiO_2 powder.

3.1.2 XRD analysis

The XRD patterns of dried PTA gel annealed at different temperatures are shown in Fig. 2. The crystallization of the TiO_2 from the PTA is influenced by many parameters, such as annealing temperature, annealing time, heating rate and atmosphere. We varied the annealing temperature and time. No diffraction peaks have been observed for the PTA gel dried at room temperature (G-RT), and the samples annealed at 120 °C (G120) and 180 °C (G180), respectively. This indicates that the samples annealed below 180 °C remain amorphous. On the other hand the XRD patterns of the G250′, G250 and G450′ give distinctive TiO_2 peaks corresponding to the anatase phase. These confirm that in our case the amorphous–anatase transformation occurred around 250 °C. As shown in Fig. 2, with increasing annealing time (G250) or annealing temperature (G450′), the peak intensity of TiO_2 increases gradually and the width of the diffraction peak becomes slightly narrower. The Scherrer equation was used to determine the average crystal sizes of the TiO_2 nanoparticles. The average size of the crystallites for samples G250′, G250 and G450′ were determined to be 20, 22 and 30 nm, respectively.

The XRD spectra of the TiO_2 layers RT, P-RT and T250 deposited from the water-based TiO_2 paste and post-treated at different conditions are given in Fig. 3. The results confirm the presence of the anatase TiO_2 phase with small amount of rutile TiO_2 phase for all three layers. The ratio between the anatase and rutile modifications of TiO_2 in all three layers remains similar to that found for TiO_2 nanopowder (P25, Degussa), which has been used as a precursor for the preparation of the TiO_2 paste. The average size of the anatase particles present in layer RT, P-RT and T250 was determined to be around 25 nm, which is the same as the average size of TiO_2 nanopowder (P25, Degussa). The addition of PTA gel (matrix) for the preparation of the paste does not significantly influence the ratio between different modifications of TiO_2 neither the average size of the crystallites in the layers, because the matrix represents solely 12.5 mol %. The spectra show also the peaks around 26.5°, 34° and 51.5°, which are characteristic for the SnO_2 based glass substrate.

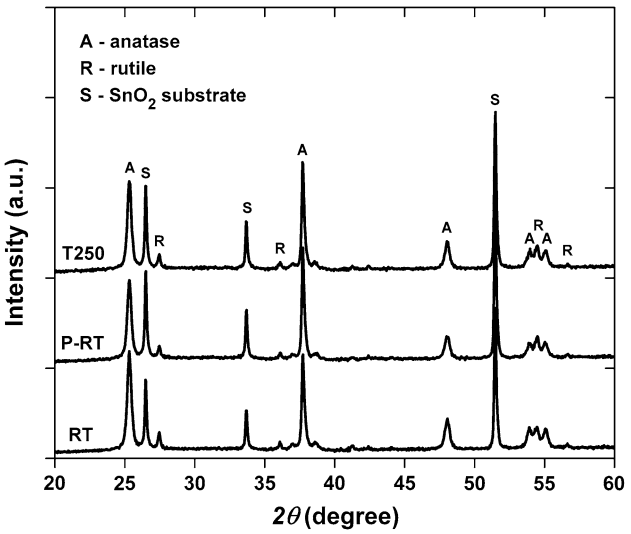

Fig. 3 The XRD patterns of layer dried at room temperature (RT), oxygen plasma-treated layer (P-RT) and layer annealed at 250 °C for 15 h (T250)

3.1.3 SEM analysis

The insight views of the TiO_2 layers RT, P-RT and T250 post-treated at different conditions showing the layers morphology are presented in Fig. 4. The SEM micrograph of the layer RT shows agglomerated TiO_2 particles coated with continues layer of PTA matrix. According to the XRD measurement the PTA matrix remains amorphous when dried at room temperature (Fig. 2, G-RT). The SEM micrographs reveal that oxygen plasma-treated layer (Fig. 4, P-RT) and layer annealed at 250 °C for 15 h (Fig. 4, T250) consist of homogeneously distributed spherical TiO_2 grains (~25 nm), which is in agreement with the average crystal size determined by XRD (Fig. 3, P-RT, T250). It is evident that the continuous PTA matrix noticed in layer RT decomposed in layer P-RT and T250. These results are well in accordance with the XRD measurement (Fig. 2), which proves that around 250 °C the amorphous-crystals transformation occurs. The results of the SEM analysis (Fig. 4, P-RT) show that the crystallization is achievable also with the oxygen plasma treatment.

3.2 Dye sensitized solar cell

The TiO_2 layers exposed to different treatment conditions were sensitized with N719 dye and evaluated in DSSCs based on electrolyte A. The thickness (d) of the TiO_2 layers and the amount of the dye molecules attached to the surface of TiO_2 layer (n_{dye}/V_{layer}) are shown in Table 1. The thickness of the layer dried at room temperature (layer RT) is 7.1 μm, while the thicknesses of all other layers are between 6.0 and 6.2 μm. The difference in thicknesses is due to the removal of the water from the TiO_2 paste during annealing/plasma treatment. In addition, the PTA matrix converts to the anatase crystals during thermal or plasma treatment process (see Sect. 3.1.2).

In the first set of experiments the dye loading/chemisorption for the TiO_2 layers treated at different temperature-time combinations are compared (Table 1, temperature treatment). For the layer RT the lowest amount of attached dye molecules per volume of the layer n_{dye}/V_{layer} i.e. 5.8×10^{-5} mol/cm^3 was found. The reason is that the continuous amorphous phase in the layer RT decreases the surface area of the TiO_2 layer. On the other hand layers T120, T180, T250′, T250 show almost no difference in dye loading (n_{dye}/V_{layer}), while the layer T450′ possesses the highest value being 8.7×10^{-5} mol/cm^3. The results of the I–V characterization (Table 1, temperature treatment) show that generally an increase in the annealing temperatures of the layers results in an increase in short-circuit density (J_{SC}), open-circuit voltage (V_{OC}) and consequently in conversion efficiency (η). As expected, the $DSSC_{RT}$ generates the lowest J_{SC} (0.68 mA/cm^2). The TiO_2 particles in the layer RT are coated with continuous amorphous phase of the PTA gel (see Sect. 3.1.3), which is reflected in smaller amount of the dye molecules attached to the layer and most likely also in a decrease of the electron transport within TiO_2 layer, both limiting the J_{SC}. Higher J_{SC}, 3.5 and 4.5 mA/cm^2, were

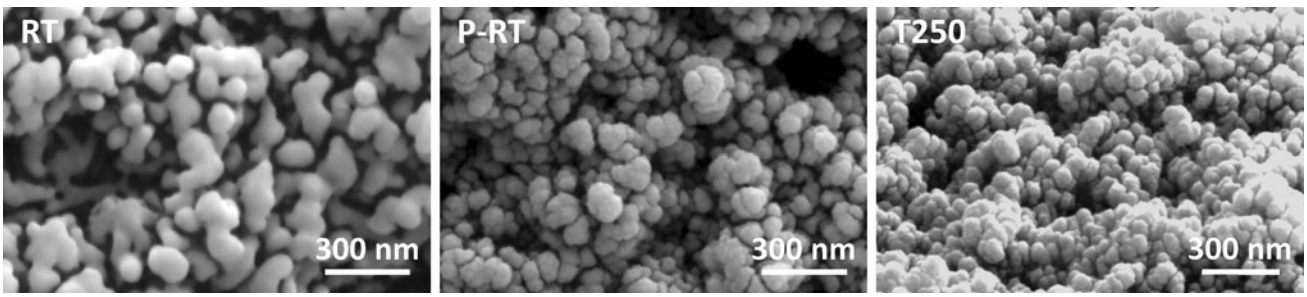

Fig. 4 The SEM micrographs showing insight view of layer dried at room temperature (RT), oxygen plasma-treated layer (P-RT) and layer annealed at 250 °C for 15 h (T250)

Table 1 The layer thickness (d), the amount of the dye molecules attached to the surface of TiO_2 layers (n_{dye}/V_{layer}), short-circuit current density (J_{SC}), open-circuit voltage (V_{OC}), fill factor (FF) and conversion efficiency (η) under STC of the DSSCs assembled with the TiO_2 layers treated at different conditions. The DSSCs are based on electrolyte A

TiO_2 layer	d (μm)	n_{dye}/V_{layer} (mol/cm^3)	J_{SC} (mA/cm^2)	V_{OC} (V)	FF (%)	η (%)
Temperature treatment						
RT	7.1	5.8×10^{-5}	0.68	0.51	60	0.2
T120	6.2	8.5×10^{-5}	3.52	0.58	66	1.4
T180	6.2	8.4×10^{-5}	4.53	0.58	63	1.7
T250′	6.1	8.4×10^{-5}	5.41	0.58	63	2.0
T250	6.1	8.5×10^{-5}	7.12	0.62	64	2.8
T450′	6.0	8.7×10^{-5}	8.51	0.63	58	3.1
Plasma treatment						
P-RT	6.2	8.0×10^{-5}	5.73	0.59	64	2.2
P120′	6.1	7.7×10^{-5}	4.13	0.58	64	1.5
P180′	6.2	7.8×10^{-5}	4.64	0.59	62	1.7
P250′	6.1	8.2×10^{-5}	6.21	0.59	61	2.2

obtained for the $DSSC_{T120}$ and $DSSC_{T180}$, respectively. According to the XRD measurement (Fig. 2) showing the crystallization of the amorphous phase to occur around 250 °C we expected that both cells ($DSSC_{T120}$ and $DSSC_{T180}$) would achieve similar current density as $DSSC_{RT}$. The reason could be the catalytic nature of the basic TiO_2 nanoparticles (Degussa P25) in the paste. This effect has been confirmed for the Pechini sol–gel based TiO_2 pastes by applying thermal analysis [35]. The presence of TiO_2 nanoparticles in the sol–gel matrix lowered the decomposition temperature of the matrix for more than 30 °C [35]. The best performance of DSSC based on electrolyte A with the efficiency of 3.1 % was realized with the layer T450′ exhibiting also the highest dye loading (Table 1, temperature treatment). Nevertheless, the $DSSC_{T250}$ shows only 10 % relatively lower conversion efficiency compared to the $DSSC_{T450'}$, although the layer in $DSSC_{T250}$ was treated at 250 °C.

In the second set of measurements, the layers exposed to the oxygen plasma treatment are compared (Table 1, plasma treatment). The variation in dye loading for all the layers exposed to the oxygen plasma treatment was within 6 %. This demonstrates that preconditioning of the TiO_2 layer with the temperature prior oxygen plasma treatment does not influence much the dye loading. The results are in accordance with the expectations, since the oxygen plasma treatment enhances the hydrophilicity on the TiO_2 surface [30, 39, 40] promoting the dye adsorption. The highest enhancement of the dye adsorption, for around 30 %, was noticed for the layer not being exposed previously to the temperature treatment (layer P-RT *vs*. RT, Table 1). On the other hand the results of the *I/V* characterization of the cells assembled with layer P-RT, P120′, P180′ and P250′ show significant difference in J_{SC}, but almost no difference in V_{OC} (Table 1, plasma treatment). The $DSSC_{P\text{-}RT}$, assembled with a layer P-RT treated solely with oxygen plasma, generates 5.7 mA/cm^2 and achieves the efficiency of 2.2 %. While the $DSSC_{P250'}$ compared to the $DSSC_{P\text{-}RT}$ shows 8 % higher J_{SC}, but the same efficiency due to the differences in the fill factor (FF). However, a significantly lower J_{SC}, for more than 20 % and consequently also lower η are noticed for $DSSC_{P120'}$ and $DSSC_{P180'}$, when compared with the $DSSC_{P\text{-}RT}$. The exact reason for this remains unknown.

The IPCE measurements of the $DSSC_{RT}$, $DSSC_{P\text{-}RT}$ and $DSSC_{T250}$ based on the electrolyte A are shown in Fig. 5. The shapes of all IPCE responses are typical for DSSC using N719 dye and iodide/triiodide based electrolyte [34]. The $DSSC_{RT}$ shows significantly smaller IPCE compared

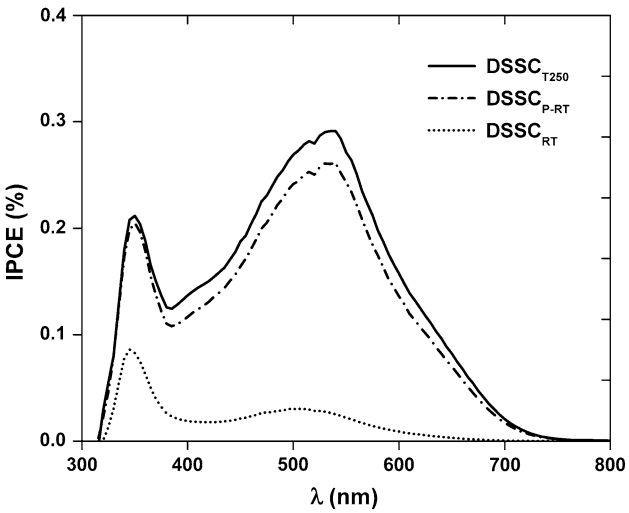

Fig. 5 The incident photon to current efficiency of $DSSC_{RT}$, $DSSC_{P\text{-}PR}$ and $DSSC_{T250}$ based on electrolyte A

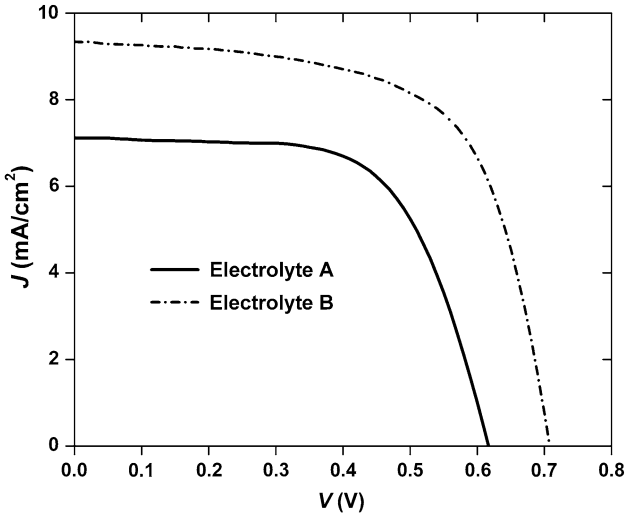

Fig. 6 The current–voltage characteristic of $DSSC_{T250}$ based on electrolyte *A* and *B*

to the $DSSC_{P\text{-}PR}$ and $DSSC_{T250}$, which is well in agreement with the measured values of J_{SC}. The AM1.5 weighted integral of the IPCE response of the $DSSC_{T250}$ is for 17 % larger compared to the $DSSC_{P\text{-}RT}$, which is in accordance with the differences in J_{SC} of the $DSSC_{T250}$ and $DSSC_{P\text{-}RT}$ being 20 %.

Figure 6 shows the *I–V* curves obtained for DSSC assembled with the layer T250 and electrolyte A and B. The cell made with electrolyte B generates 9.3 mA/cm^2, 0.71 V and consequently achieves the efficiency of 4.2 %. The results indicate that the DSSC based on acetonitrile electrolyte (Electrolyte B) generates for 23 % more J_{SC} when compared with the cell made with the electrolyte A. Overall conversion efficiencies for layer T250 with electrolytes A and B were 2.8 % and 4.2 %, respectively.

4 Conclusions

We report on the simple preparation of the water-based TiO_2 paste enabling temperature curing $\leq$250 °C or oxygen plasma treatment. The paste is based on commercial TiO_2 nanopowder P25 and sol–gel matrix achieved by mixing $Ti(OiPr)_4$ and H_2O_2 forming a complexing gel called peroxotitanic acid (PTA). The PTA matrix in the paste converts to anatase TiO_2 crystallites and attaches to the basic TiO_2 nanoparticles P25 upon annealing process or oxygen plasma treatment. The results confirm that the PTA gel transformation occurs around 250 °C, but in the presence of TiO_2 nanoparticles P25 i.e. in the paste the crystallization of the PTA matrix starts already at 120 °C.

On the other hand, the results indicate that oxygen plasma treatment of TiO_2 layers could efficiently replace temperature curing and avoid time-consuming process. In this study, the oxygen plasma treated layer P-RT in DSSC shows comparable performances as the layer T250′ annealed at 250 °C for 1 h.

The highest efficiency of DSSCs was achieved with the TiO_2 layers T250 cured at 250 °C for 15 h. The efficiencies of the $DSSCs_{T250}$ assembled with ionic liquid-based electrolyte (Electrolyte A) and acetonitrile based electrolyte (Electrolyte B) were 2.8 % and 4.2 %, respectively.

Acknowledgments The authors gratefully acknowledge the group of Prof. Miran Mozetič at the Jožef Stefan Institute (IJS, Ljubljana, Slovenia) for the oxygen plasma treatment. Jožko Fišer (IJS) is acknowledged for measurements of the layers' thicknesses and Jože Buh (IJS) for the SEM analyses of the TiO_2 layers. M. H. is grateful for the financial support given by the Slovenian Research Agency (Z2–4152–1538). The work was also partially funded by the Slovenian Research Agency under the P2–0197 program.

References

1. O'Regan B, Grätzel M (1991) A low–cost, high efficiency solar cells based on dye-sensitized colloidal TiO_2 films. Nature 353:737–740
2. Hinsch A, Veurman W, Brandt H, Loayza Aguirre R, Bialecka K, Flarup Jensen K (2012) Worldwide first fully up-scaled fabrication of 60 × 100 cm^2 dye solar module prototypes. Prog Photovolt Res Appl 20:698–710
3. Hočevar M, Opara Krašovec U, Bokalič M, Topič M, Veurman W, Brandt H, Hinsch A (2013) Sol-gel based TiO_2 paste applied in screen-printed dye-sensitized solar cells and modules. J Ind Eng Chem 19:1464–1469
4. Hočevar M, Berginc M, Opara Krašovec U, Topič M (2012) In: Aparicio M, Jitianu A, Klein LC (eds) Sol–gel processing for conventional and alternative energy. Springer, New York
5. Hagfeldt A, Boschloo G, Sun L, Kloo L, Pettersson H (2010) Dye-sensitized solar cells. Chem Rev 110:6595–6663
6. Miettunen K, Halme J, Lund P (2013) Metallic and plastic dye solar cells. WIREs Energy Environ 2:104–120
7. Lee KM, Hsu YC, Ikegami M, Miyasaka T, Thomas KRJ, Lin JT, Ho KC (2011) Co-sensitization promoted light harvesting for plastic dye-sensitized solar cells. J Power Sources 196:2416–2421
8. Weerasinghea HC, Sirimanne PM, Franks GV, Simon GP, Cheng YB (2010) Low temperature chemically sintered nano-crystalline TiO_2 electrodes for flexible dye-sensitized solar cells. J Photochem Photobiol A Chem 213:30–36
9. Kalyanasundaram K (2010) Dye-sensitized solar cells. EPFL Press, Lausanne
10. Yamaguchi T, Tobe N, Matsumoto D, Nagai T, Arakawa H (2010) Highly efficient plastic-substrate dye-sensitized solar cells with validated conversion efficiency of 7.6%. Sol Energ Mat Sol C 94:812–816
11. Yella A, Lee H-W, Tsao HN, Yi C, Chandiran AK, Nazeeruddin MK, Diau EW-G, Yeh C-Y, Zakeeruddin SM, Grätzel M (2011) Porphyrin-sensitized solar cells with cobalt (II/III)–based redox electrolyte exceed 12 percent efficiency. Science 334:629–634
12. He X-L, Liu M, Yang G-J, Yao H-L, Fan S-Q, Li C-J (2013) Photovoltaic performance degradation and recovery of the flexible dye-sensitized solar cells by bending and relaxing. J Power Sources 226:173–178
13. Yen W-H, Hsieh C-C, Hung C-Y, Wang H-W, Tsui M-C (2010) Flexible TiO_2 working electrode for dye-sensitized solar cells. J Chin Chem Soc 57:1162–1166

14. Lin L-Y, Lee C-P, Tsai K-W, Yeh M-H, Chen C-Y, Vittal R, Wu C-G, Ho K-C (2012) Low-temperature flexible Ti/TiO_2 photoanode for dye-sensitized solar cells with binder-free TiO_2 paste. Prog Photovolt Res Appl 20:181–190
15. Gutiérrez-Tauste D, Zumeta I, Vigil E, Hernández-Fenollosa MA, Domènech X, Ayllón JA (2005) New low-temperature preparation method of the TiO_2 porous photoelectrode for dye-sensitized solar cells using UV irradiation. J Photochem Photobiol A Chem 175:165–171
16. Zhang D, Yoshida T, Minoura H (2003) Low-temperature fabrication of efficient porous titania photoelectrodes by hydrothermal crystallization at the solid/gas interface. Adv Mater 15:814–817
17. Li Y, Yoo K, Lee D-K, Kim JH, Park N-G, Kim K, Ko MJ (2010) Highly bendable composite photoelectrode prepared from TiO_2/polymer blend for low temperature fabricated dye-sensitized solar cells. Curr Appl Phys 10:E171–E175
18. Lindström H, Holmberg A, Magnusson E, Malmqvist L, Hagfeldt A (2001) A new method to make dye-sensitized nanocrystalline solar cells at room temperature. J Photochem Photobiol A Chem 145:107–112
19. Lindström H, Holmberg A, Magnusson E, Lindquist SE, Malmqvist L, Hagfeldt A (2001) A new method for manufacturing nanostructured electrodes on plastic substrates. Nano Lett 1:97–100
20. Dürr M, Schmid A, Obermaier M, Rosselli S, Yasuda A, Nelles G (2005) Low-temperature fabrication of dye-sensitized solar cells by transfer of composite porous layers. Nat Mater 4:607–611
21. Ge L, Xu MX, E L, Tian YM, Fang HB (2005) Preparation of TiO_2 thin films using inorganic peroxo titanic complex and autoclaved sols as precursors. Key Eng Mater 280:809–812
22. Modic M, Junkar I, Vesel A, Mozetič M (2012) Aging of plasma treated surfaces and their effects on platelet adhesion and activation. Surf Coat Technol 213:98–104
23. De Geyter N, Morent R, Leys C (2008) Influence of ambient conditions on the ageing behaviour of plasma-treated PET surfaces. Nucl Instrum Methods Phys Res B 266:3086–3090
24. Mozetič M (2011) Extremely non-equilibrium oxygen plasma for direct synthesis of metal oxide nanowires on metallic substrates. J Phys D Appl Phys 44:1–9
25. Mancini SD, Nogueira AR, Rangel EC, Da Cruz NC (2013) Solid-state hydrolysis of postconsumer polyethylene terephthalate after plasma treatment. J Appl Polym Sci 127:1989–1996
26. Eleršič K, Junkar I, Modic M, Zaplotnik R, Vesel A, Cvelbar U (2011) Modification of surface morphology of graphite by oxygen plasma treatment. Mater Tehnol 45:232–239
27. Liu R, Yang WD, Qiang LS (2012) Enhanced efficiency for dye-sensitized solar cells using a surface-treated photo-anode. J Power Sources 199:418–425
28. Li Y, Ding JN, Yuan NY, Bai L, Hu HW, Wang XQ (2013) The influence of surface treatment on dye-sensitized solar cells based on TiO_2 nanofibers. Mater Lett 97:74–77
29. Tak Kim J, Ho Kim S (2011) Surface modification of TiO_2 electrode by various over-layer coatings and O_2 plasma treatment for dye sensitized solar cells. Sol Energ Mat Sol C 95:336–339
30. Wang J, Lin ZQ (2010) Dye sensitized TiO_2 nanotube solar cells with markedly enhanced performance via rational surface engineering. Chem Mater 22:579–584
31. Berginc M, Opara Krašovec U, Hočevar M, Topič M (2008) Performance of dye-sensitized solar cells based on Ionic liquids: effect of temperature and iodine concentration. Thin Solid Films 516:7155–7159
32. Hočevar M, Opara Krašovec U, Berginc M, Dražić G, Hauptman N, Topič M (2008) Development of TiO_2 pastes modified with Pechini sol-gel method for high efficiency dye-sensitized solar cell. J Solgel Sci Technol 48:156–162
33. Zaplotnik R, Vesel A, Mozetic M (2013) A powerful remote source of O atoms for the removal of hydrogenated carbon deposits. J Fusion Energy 32:78–87
34. Hočevar M, Opara Krašovec U, Berginc M, Topič M (2010) One step preparation of TiO_2 layer for high efficiency dye-sensitized solar cell. Acta Chim Slov 57:405–409
35. Drev M, Opara Krašovec U, Hočevar M, Berginc M, Kržmanc Maček M, Topič M (2011) Pechini based titanium sol as a matrix in TiO_2 pastes for dye-sensitized solar cell application. J Solgel Sci Technol 59:245–251
36. Hočevar M, Berginc M, Topič M, Opara Krašovec U (2010) Sponge-like TiO_2 layers for dye-sensitized solar cells. J Solgel Sci Technol 53:647–654
37. Ge L, Xu MX, Sun M, Fang HB (2006) Low-temperature synthesis of photocatalytic TiO_2 thin film from aqueous anatase precursor sols. J Solgel Sci Technol 38:47–53
38. Ge L, Xu MX (2007) Fabrication and characterization of TiO_2 photocatalytic thin film prepared from peroxo titanic acid sol. J Solgel Sci Technol 43:1–7
39. Mor GK, Shankar K, Paulose M, Varghese OK, Grimes CA (2006) Use of highly-ordered TiO_2 nanotube arrays in dye-sensitized solar cells. Nano Lett 6:215–218
40. Tsoi S, Fok E, Sit JC, Veinot JGC (2004) Superhydrophobic, high surface area, 3-D SiO_2 nanostructures through siloxane-based surface functionalization. Langmuir 20:10771–10774